



Nonlinear optical properties of tungstate fluorophosphate glasses

E. L. Falcão-Filho, Cid B. de Araújo, C. A. C. Bosco, L. H. Acioli, G. Poirier, Y. Messaddeq, G. Boudebs, and M. Poulain

Citation: *Journal of Applied Physics* **96**, 2525 (2004); doi: 10.1063/1.1758309

View online: <http://dx.doi.org/10.1063/1.1758309>

View Table of Contents: <http://scitation.aip.org/content/aip/journal/jap/96/5?ver=pdfcov>

Published by the [AIP Publishing](#)



Re-register for Table of Content Alerts

Create a profile.



Sign up today!



Nonlinear optical properties of tungstate fluorophosphate glasses

E. L. Falcão-Filho, Cid B. de Araújo,^{a)} C. A. C. Bosco, and L. H. Acioli
Departamento de Física, Universidade Federal de Pernambuco, 50670-901 Recife, PE, Brazil

G. Poirier and Y. Messaddeq
Instituto de Química, UNESP, 14801-970 Araraquara, SP, Brazil

G. Boudebs
Laboratoire des Propriétés Optique des Matériaux et Applications, Université d'Angers, 49045 Angers Cedex 01, France

M. Poulain
Laboratoire des Matériaux Photoniques, Université de Rennes I, Rennes, France

(Received 3 March 2004; accepted 14 April 2004)

The optical nonlinearity of tungstate fluorophosphate glasses, synthesized in the NaPO₃-BaF₂-WO₃ system, was investigated through experiments based on the third-order susceptibility, $\chi^{(3)}$. Nonlinear (NL) refraction and NL absorption measurements in the picosecond regime were performed using the Z-scan technique at 532 nm. NL refractive index, $n_2 \propto \text{Re } \chi^{(3)}$, ranging from $0.4 \times 10^{-14} \text{ cm}^2/\text{W}$ to $0.6 \times 10^{-14} \text{ cm}^2/\text{W}$ were determined. The two-photon absorption coefficient, $\alpha_2 \propto \text{Im } \chi^{(3)}$, for excitation at 532 nm, vary from 0.3 to 0.5 cm/GW. Light induced birefringence experiments performed in the femtosecond regime indicate that the response time of the nonlinearity at 800 nm is faster than 100 fs. The experiments show that $\chi^{(3)}$ is enhanced when the WO₃ concentration increases and this behavior is attributed to the hyperpolarizabilities associated to W–O bonds. © 2004 American Institute of Physics. [DOI: 10.1063/1.1758309]

I. INTRODUCTION

Tungstate fluorophosphate (TFP) glasses, have been considered as promising materials for optical limiting and as host materials for fluorescence studies of rare earth ions. First, nonlinear (NL) absorption measurements¹ have shown that these glasses present a large two-photon absorption (TPA) coefficient α_2 which depends on the relative amount of tungsten oxide WO₃ in the samples. Values of α_2 up to 11 cm/GW were determined at 660 nm, using nanosecond laser pulses. Further, spectroscopic properties of Tm³⁺ doped TFP were investigated.² Transition probabilities, branching ratios, and radiative lifetimes associated to the Tm³⁺ levels were determined. The lifetimes measured were understood considering radiative relaxation, multiphonon processes, and energy transfer among Tm³⁺ ions. A mechanism was also proposed to describe the origin of the frequency upconversion process observed.

More recently, structural characterizations were performed by x-ray absorption spectroscopy (XANES) at the tungsten L_I and L_{III} absorption edges and by Raman spectroscopy.^{3,4} XANES investigations showed that the tungsten atoms are sixfold coordinated (WO₆ octahedrons) and that the glasses do not contain WO₄ tetrahedrons. Raman spectroscopy allowed to identify a break in the linear phosphate chains when increasing WO₃ concentration. Also, formation of P–O–W bonds was observed which indicates the modifier behavior of WO₆ octahedrons in the glass network. Based on the XANES data it had identified the presence of

W–O–W bridging bonds in the samples with WO₃ concentration larger than 30% molar, due to the formation WO₆ clusters.

The aim of this paper is to report experimental results on TFP glasses using picosecond and femtosecond pulsed lasers. The NL refraction and NL absorption properties of TFP glasses were studied for various WO₃ concentrations using the Z-scan technique^{5,6} at 532 nm and 1064 nm. NL refractive indices, $n_2 \propto \text{Re } \chi^{(3)}$, ranging from $0.4 \times 10^{-14} \text{ cm}^2/\text{W}$ to $0.6 \times 10^{-14} \text{ cm}^2/\text{W}$ at 532 nm were determined. The two-photon absorption coefficient, $\alpha_2 \propto \text{Im } \chi^{(3)}$, vary from 0.3 to 0.5 cm/GW at 532 nm. Light induced birefringence experiments at 800 nm using the Kerr gate technique⁷ have shown that the response time of the nonlinearity is faster than 100 fs. The results for all wavelengths indicate an increase of the third-order susceptibility $\chi^{(3)}$ with the increase of WO₃ concentration. Based on the data from XANES and Raman spectroscopy^{3,4} we attribute the behavior of $\chi^{(3)}$ to the hyperpolarizability associated to W–O bonds. A semiempirical model was used to estimate the NL refractive index at 800 nm. The results are in agreement with the experimental data.

II. EXPERIMENTAL DETAILS

The TFP glass samples were synthesized by a conventional method. The powdered starting materials were: tungsten oxide WO₃ from Alpha (99.8% pure); sodium polyphosphate NaPO₃ from Acros (99+% pure); and barium fluoride BaF₂ from Aldrich (99.8% pure).

In a first step the powders were mixed and heated at 400 °C for 1 h to remove water and adsorbed gases. Then a batch was melted at a temperature ranging from 850 °C to

^{a)} Author to whom correspondence should be addressed; fax: +55-81 3271 0359; electronic mail: cid@df.ufpe.br

TABLE I. Samples compositions, characteristic temperatures and thermal stability range of the TFP glasses. T_g is the glass transition temperature and T_x refers to the onset of crystallization. The estimated error on the temperature measurements is ± 2 K.

Samples	Glass compositions (mol %)			Characteristic temperatures (K)		
	NaPO ₃	BaF ₂	WO ₃	T_g	T_x	$T_x - T_g$
NBW20	64	16	20	320	584	264
NBW30	56	14	30	370	>600	>230
NBW40	48	12	40	418	>600	>182
NBW50	40	10	50	465	>600	>135

1200 °C, depending on the WO₃ content. The liquid was kept at 1200 °C for 15–60 min to ensure homogenization and fining. Finally the melt was cooled in a brass mold preheated at the glass transition temperature. Annealing was implemented at this temperature for several hours in order to minimize mechanical stress resulting from thermal gradients upon cooling.

A set of samples with various WO₃ concentrations were prepared according to the following composition in mol %: $(80 - 0.8x)\text{NaPO}_3 - (20 - 0.2x)\text{BaF}_2 - x\text{WO}_3$, with $x = 20, 30, 40$, and 50. The glass transition temperature T_g , the onset of crystallization T_x , and the thermal stability range $T_x - T_g$, are indicated in Table I. More details on the samples preparation are presented elsewhere.^{3,4} Bulk samples with dimensions of $15 \times 15 \times 3$ mm³ were cut and polished for the optical measurements.

Measurements of the linear refractive index at 633 nm and 1550 nm were performed using the prism coupler technique. Low intensity optical transmission was measured using spectrophotometers operating from the midinfrared to the near ultraviolet.

The light source used in the NL optics experiments at 1064 nm and 532 nm was a Q-switched and mode-locked Nd:yttrium aluminum garnet (YAG) laser delivering bursts of pulses of ≈ 100 ps duration at 1064 nm. The second harmonic radiation obtained using a KTP crystal was employed for measurements at 532 nm with pulses of ≈ 80 ps duration. Single pulses at low repetition rate (10–100 Hz) were selected using a pulse extraction system. For the experiments at 800 nm a Ti:Sapphire laser system, delivering ≈ 100 fs pulses at a repetition rate of 82 MHz, was employed.

III. RESULTS AND DISCUSSION

Figure 1 shows that the refractive index n_0 of the TFP glass measured at 633 nm and 1550 nm increases linearly when the concentration of tungsten oxide is increased. The enhancement of n_0 with the WO₃ concentration is expected because of the large polarizability of the tungsten atoms.

The low intensity optical absorption of the samples was recorded from $30\,000$ cm⁻¹ in the ultraviolet to 2000 cm⁻¹ in the infrared. The transmission is limited by the optical band gap at short wavelength and by multiphonon absorption in the infrared. The results for different glass compositions are presented in Fig. 2 which shows a redshift of the optical band gap when the WO₃ concentration increases. A large absorption band, observed around 2600 cm⁻¹, is attributed to

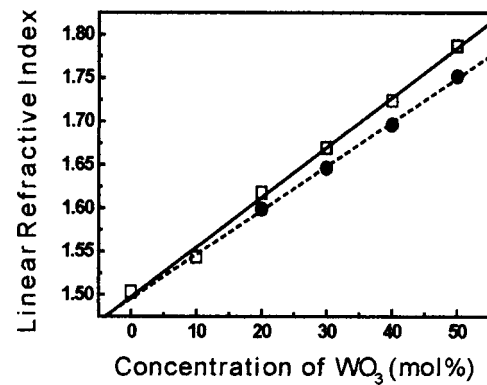


FIG. 1. Refractive index vs the WO₃ content. Measurements at 633 nm (□) and at 1550 nm (●).

residual hydroxyl groups and multiphonon absorption of the O–P–O chains in the polyphosphate structure.^{3,4}

NL refraction and NL absorption were investigated using the Z-scan technique⁵ at 1064 nm and 532 nm. To implement the Z-scan technique the laser beam was focused by a 10 cm focal distance lens. The sample was mounted in a translation stage to be moved in the focus region, along the beam propagation direction (Z axis). Negative values of Z correspond to locations of the sample between the focusing lens and its focal plane. The output of a slow detector, placed in the far-field region with an adjustable aperture in front of it, was fitted to a boxcar integrator for signal analysis. The aperture radius r_a is related to the aperture linear transmittance which is given by $S = 1 - \exp(-2r_a^2/w_a^2)$, with w_a denoting the beam

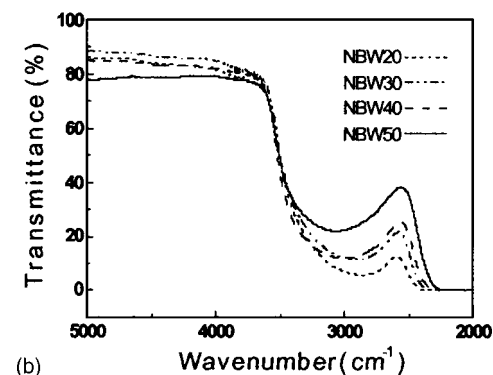
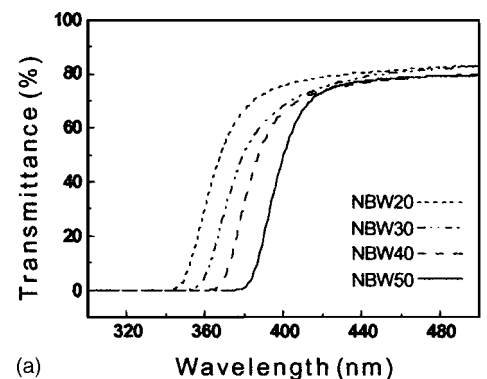


FIG. 2. Ultraviolet and infrared transmission edges as a function of the glass composition. Tungsten oxide concentration: (1) 20%; (2) 30%; (3) 40%; (4) 50%; Samples thicknesses, 3 mm.

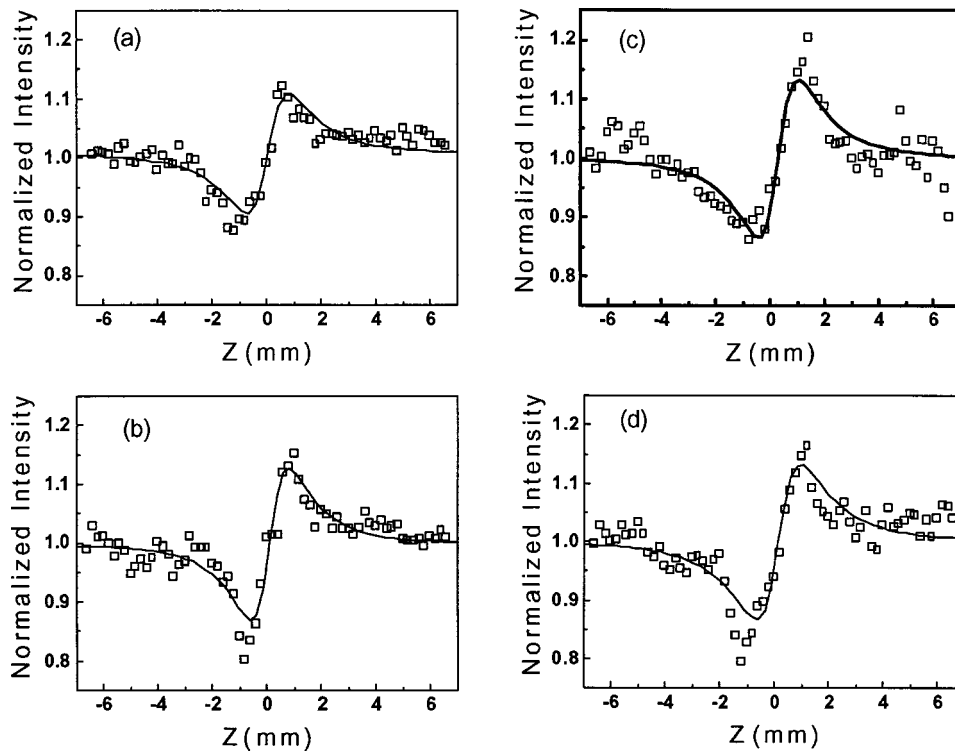


FIG. 3. Closed aperture Z-scan traces for various WO₃ concentrations in mol %: (a) 20; (b) 30; (c) 40; (d) 50. Excitation wavelength, 532 nm.

radius at the aperture position for low incident power. n_2 is determined measuring the variation of the transmitted beam intensity in the closed aperture Z-scan scheme ($S < 1$) for high incident power. On the other hand, when the beam passing through the sample is unblocked (open aperture scheme: $S = 1$), and all transmitted light is recorded as a function of Z , it is possible to determine α_2 . To obtain a better signal-to-noise ratio a reference channel was used as in Ref. 6.

Figures 3(a)–3(d) show typical closed aperture Z-scan traces obtained at 532 nm. The total change in the normalized transmittance, for $S < 1$, is given by $\Delta T = 0.406kL_{\text{eff}}n_2I_{\text{pump}}$, where I_{pump} is the excitation peak intensity, $k = 2\pi/\lambda$, $L_{\text{eff}} = [1 - \exp(-\alpha_0 L)]/\alpha_0$, L is the sample length, and λ is the excitation light wavelength. A self-focusing nonlinearity is observed and enhancement of n_2 for larger WO₃ concentration is displayed. Figures 4(a)–4(d) show the results for the open-aperture Z-scan experiments at 532 nm where the traces profiles indicate increasing NL absorption for increasing values of WO₃ concentration. Each data point in Figs. 3 and 4 represents the average of 20 shots and four scans. The solid lines are the best-fit curves obtained using the procedure of Ref. 5. Carbon disulfide was used as a reference sample with $n_2 = 3.1 \times 10^{-14} \text{ cm}^2/\text{W}$.⁵ The values of n_2 and α_2 , determined with an estimated error of 20%, are indicated in Table II.

Z-scan experiments performed at 1064 nm did not show relevant NL behavior. From the experiments we estimated the value of $n_2 \approx 0.1 \times 10^{-14} \text{ cm}^2/\text{W}$ for the sample containing 50% of WO₃. The NL parameters of the other samples could not be measured with the sensitivity available and we inferred that the values of n_2 and α_2 for WO₃ concentration $x < 50\%$ are smaller than $0.07 \times 10^{-14} \text{ cm}^2/\text{W}$ and $0.02 \text{ cm}/\text{GW}$, respectively.

The temporal response of the TFP glasses and the value of n_2 at 800 nm were evaluated using a Kerr gate setup with the sample placed between crossed polarizers.⁷ For these experiments the light beam from the Ti:Sapphire laser was split into two beams with 1:10 intensities ratio. The stronger (pump) beam induces a refractive index change in the sample, $\Delta n(t) = n_2 I_{\text{pump}}(t)$, where $I_{\text{pump}}(t)$ is the pump beam intensity. The probe beam with its polarization set at 45° with respect to the pump beam polarization is used to investigate the dynamics of $\Delta n(t)$. Both beams were focused by a 10 cm focal length lens and the intensity of the pump beam at the focus was $\sim 2 \text{ GW}/\text{cm}^2$.

A small fraction of the probe beam intensity leaks out the polarizer analyzer located in front of the photodiode which allows for homodyne detection of $\Delta n(t)$. When the pump beam is present, the probe beam polarization is rotated due to the pump beam induced birefringence with a dynamical behavior that depends on the material response time and the laser pulse duration.⁷ Consequently, a larger fraction of the probe beam intensity reaches the photodiode. A lock-in amplifier provides a temporally averaged signal $S(\tau) \propto \langle \Delta n(t) \times I_{\text{probe}}(t + \tau) \rangle$ for each delay time, τ , between pump and probe pulses spatially overlapped at the sample position. The signal $S(\tau)$ was monitored by scanning a delay line which allows for different values of τ .

The behavior of $S(\tau)$ for samples with different WO₃ concentrations is shown in Fig. 5(a). For the assumed hyperbolic secant pulse shape, the symmetric correlation signal of width equal to $\approx 160 \text{ fs}$ implies that the samples have a response faster than 100 fs. This means that the nonlinearity originates mainly from electronic processes. $S(\tau)$ presents a linear dependence versus the pump laser power, as expected for a homodyne Kerr shutter signal. Variation of the samples'

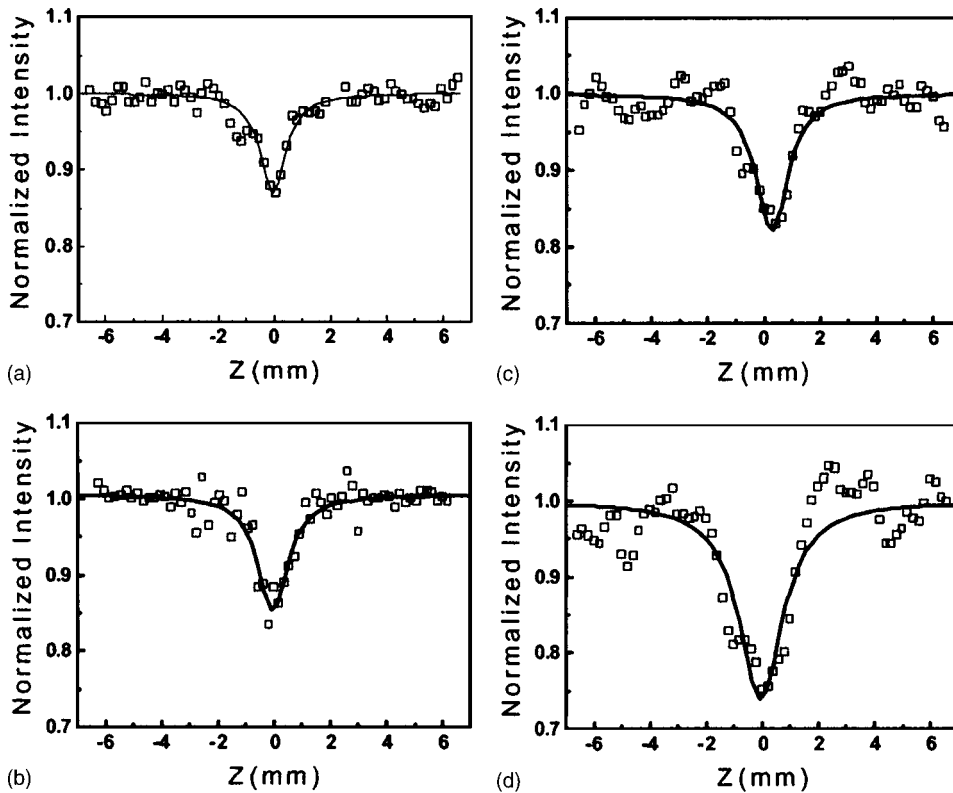


FIG. 4. Open aperture Z-scan traces for various WO₃ concentrations in mol %: (a) 20; (b) 30; (c) 40; (d) 50. Excitation wavelength, 532 nm.

transmittance as a function of the pump beam intensity was not observed in the experiments at 800 nm, which implies that the TPA coefficient is below our detection limit (<0.01 cm/GW). This is because twice the photon energy is smaller than the optical band gap.

The magnitude of $|n_2|$ is obtained by comparison with the fused silica NL refractive index of 2.2×10^{-16} cm²/W (Ref. 8) which was used as a calibration standard. The values of $|n_2|$ for excitation at 800 nm are plotted in Fig. 5(b) where the dependence with the WO₃ concentration is demonstrated. A comparison between the results for n_2 in 532 nm and 800 nm indicates that the values in the visible are larger by more than 100% which is attributed to the smaller green laser frequency detuning with respect to the samples' band gap. Comparing the results for α_2 in the picosecond regime with the ones reported in the nanosecond regime,¹ we observe that the values of Ref. 1 are about one-order of magnitude larger than the results obtained in the present experiments. Similar relative behavior of TPA coefficients for nanosecond and picosecond excitation was reported by other authors for different materials.^{9,10} This is normally due to contributions of free carriers or long lived impurity states which are more important in nanosecond experiments.

TABLE II. Nonlinear parameters determined by the Z-scan technique at 532 nm.

Sample	n_2 (10^{-14} cm ² /W)	α_2 (cm/GW)
NBW20	0.40 ± 0.08	0.30 ± 0.06
NBW30	0.40 ± 0.08	0.40 ± 0.08
NBW40	0.45 ± 0.09	0.45 ± 0.09
NBW50	0.60 ± 0.11	0.50 ± 0.10

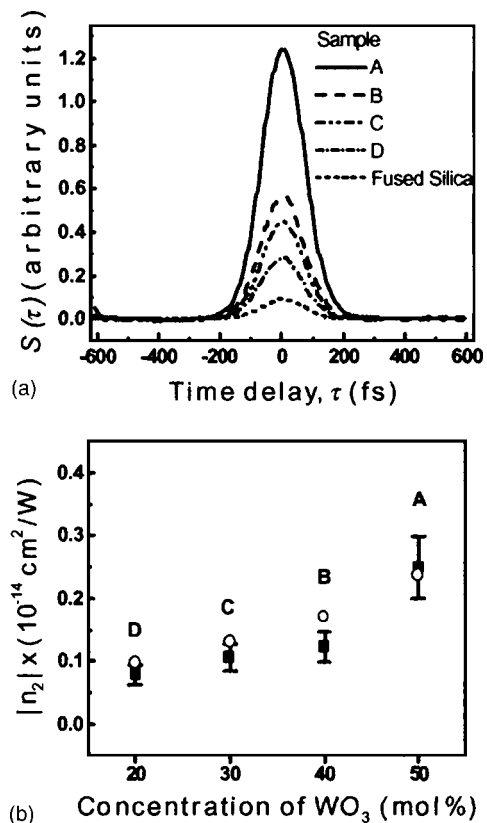


FIG. 5. Kerr shutter results at 800 nm (a) Temporal evolution of the signal (the curve for fused silica is also presented to illustrate the sensitivity of the setup); (b) Nonlinear refractive index versus WO₃ concentrations: (■) experimental results; (○) theory. The tungsten oxide content of samples A–D is indicated in (b).

A common feature to all measurements presented here is the increase of the NL parameters when the concentration of WO_3 is increased. This is attributed to the presence of W–O–W bonds demonstrated in Refs. 3 and 4 which influence the NL behavior of the samples due to the high hyperpolarizability associated to the W–O bond. We already recall that it is already reported for other glasses that the introduction of transition metals, including tungsten, may enhance the NL properties of a material.¹¹

Using a simple model based on a classical nonlinear oscillator [Boiling, Glass, and Owyong (BGO)-model],¹² it was possible to estimate values for n_2 which are in agreement with the experimental data. In the BGO-model the third-order hyperpolarizability is assumed to be proportional to the linear polarizability squared and the optical dispersion of the medium is determined by only one resonance at $\hbar\omega_0$. The harmonic incident light field is supposed to be far from resonance ($\omega \ll \omega_0$) and the optical properties of the medium are considered to be related to the tungsten ions. However, nuclear motions are not considered because their contribution for the nonlinearity is estimated $\leq 15\%$ for heavy-metal oxide glasses.¹³ Hence, the NL refractive index in the BGO-model, written in Gaussian units, is given by

$$n_2(esu) = \frac{(n_0(\lambda)^2 + 2)^2 (n_0(\lambda)^2 - 1)^2}{48\pi n_0(\lambda) \hbar \omega_0} \times \frac{(gs)}{(Ns)}, \quad (1)$$

where N is the tungsten ions density, s is the effective oscillator strength, g is a dimensionless parameter given by $g = \mu s \hbar / m \omega_0^3$, where μ is the anharmonic force constant, $(2\pi\hbar)$ is the Planck's constant, and m is the electron mass. The linear refractive index for light wavelength λ is denoted by $n_0(\lambda)$ and, according to Ref. 12, it is given by

$$\frac{4\pi}{3} \frac{(n_0(\lambda)^2 + 2)}{(n_0(\lambda)^2 - 1)} = \frac{\omega_0^2 - \omega^2}{(e^2/m)(Ns)}, \quad (2)$$

where e is the electron charge in Gaussian units.

The parameters Ns and ω_0 in Eq. (2) can be obtained from the values of n_0 ($\lambda=633$ nm) and n_0 ($\lambda=1550$ nm) given in Fig. 1 for each sample. Then, the values obtained for Ns and ω_0 are introduced in Eq. (1) to determine n_2 . The parameter $gs=3$ was used because it is the appropriate value for oxides according to Ref. 12.

The theoretical results obtained for n_2 at 800 nm are shown in Fig. 5(b). The value of n_0 ($\lambda=800$ nm) was determined using Eq. (2) with the values of (Ns) and ω_0 obtained for each sample. The agreement with the experimental values is very good although the results were determined using a fitting procedure.

IV. CONCLUSION

In summary, the third-order nonlinearity of tungstate fluorophosphate glasses have been studied for different WO_3

concentration. The two-photon absorption coefficient α_2 increases when the WO_3 concentration is increased. Large values of α_2 at 532 nm were obtained that makes these glasses useful for optical limiting in the picosecond regime as well as in the nanosecond regime. A NL response faster than 100 fs was characterized for excitation at 800 nm. The NL refractive index also increases when the WO_3 concentration is increased but it does not assume very large values. However, at 800 nm, TFP glasses present a reasonable figure-of-merit, $T=2\alpha_2\lambda/n_2$, for all-optical switching. In fact, considering $\alpha_2 < 0.01$ cm/GW and $n_2 \approx 0.25 \times 10^{-14}$ cm²/W, we obtain $T < 0.64$ which satisfy very well the accepted criteria.¹⁴

It is important to notice that TFP glasses have other interesting properties. For example, they are photosensitive when exposed to light at 350 nm and this phenomenon is reversible by thermal treatment. Also several meters of optical fibers have already been prepared with no evidence of crystallization. The TFP glasses are extremely easy to prepare and are not toxic as opposed to other glasses presenting large two-photon absorption coefficients such as chalcogenide glasses.

ACKNOWLEDGMENTS

We acknowledge financial support by the Brazilian Conselho Nacional de Desenvolvimento Científico e Tecnológico (CNPq) and Fundação de Amparo à Ciência e Tecnologia do Estado de Pernambuco (FACEPE). We also thank B. J. P. da Silva for cutting and polishing the samples.

- ¹G. Poirier, C. B. de Araújo, Y. Messaddeq, S. J. L. Ribeiro, and M. Poulain, *J. Appl. Phys.* **91**, 10221 (2002).
- ²G. Poirier, V. A. Jerez, C. B. de Araújo, Y. Messaddeq, S. J. L. Ribeiro, and M. Poulain, *J. Appl. Phys.* **93**, 1493 (2003).
- ³G. Poirier, Ph.D. thesis, Université de Rennes 1, 2003.
- ⁴G. Poirier, Y. Messaddeq, S. J. L. Ribeiro, and M. Poulain, *Structural Study of Tungstate Fluorophosphate Glasses by Raman and X-ray absorption spectroscopy* (submitted).
- ⁵M. Sheik-Bahae, A. A. Said, T. H. Wei, D. J. Hagan, and E. W. Van Stryland, *IEEE J. Quantum Electron.* **QE-26**, 760 (1990).
- ⁶H. Ma, A. S. L. Gomes, and C. B. de Araújo, *Appl. Phys. Lett.* **59**, 2666 (1991).
- ⁷Y. R. Shen, *The Principles of Nonlinear Optics* (Wiley, New York, 1984).
- ⁸R. De Salvo, A. A. Said, D. J. Hagan, E. W. Van Stryland, and M. Sheik-Bahae, *IEEE J. Quantum Electron.* **32**, 1324 (1996).
- ⁹T. F. Bogges, Jr., A. L. Smirl, S. C. Moss, I. A. Boyd, and E. W. Van Stryland, *IEEE J. Quantum Electron.* **QE-21**, 488 (1985).
- ¹⁰B. L. Justus, A. J. Campilo, D. G. Hendershot, and D. K. Gaskill, *Opt. Commun.* **103**, 405 (1993).
- ¹¹S. H. Kim and T. Yoko, *J. Am. Ceram. Soc.* **78**, 1061 (1995).
- ¹²N. L. Boiling, A. J. Glass, and A. Owyong, *IEEE J. Quantum Electron.* **QE-14**, 601 (1978).
- ¹³I. Kang, S. Smolorz, T. Krauss, F. Wise, B. G. Aitken, and N. F. Borrelli, *Phys. Rev. B* **54**, R12641 (1996).
- ¹⁴G. I. Stegeman, in *Nonlinear Optics of Organic Molecules and Polymers*, edited by H. S. Nalva and S. Miyata (CRC, Boca Raton, FL, 1997), p. 799.